Electromagnetically induced transparency and Autler–Townes effect in a generalized Λ-system: A five-level model

[1] Żaba A., [1] Cao Long V., [2] Głódź M., [3] Paul-Kwiek E., [2] Kowalski K., [2] Szonert J., [1] Woźniak D. and [4] Gateva S.

[1] Quantum Optics and Engineering Division, Institute of Physics, University of Zielona Góra, Prof. Z. Szafrana 4a, 65-516 Zielona Góra, Poland, e-mail: vanlongcao@yahoo.com
[2] Institute of Physics, Polish Academy of Sciences, Al. Lotników 32/46, 02-668 Warsaw, Poland, e-mail: glodz@ifpan.edu.pl
[3] Institute of Physics, Pomeranian University in Słupsk, Arciszewskiego 22b, 76-200 Słupsk, Poland, e-mail: ewa@apsl.edu.pl
[4] Institute of Electronics, Bulgarian Academy of Sciences, Tsarigradsko Chaussee 72, 1784 Sofia, Bulgaria: sanka@gbg.bg

Received: 09.04.2013

Abstract. We calculate electric susceptibility of a laser-dressed atomic medium. The model adopted in this work refers to the experiment with cold ^{85}Rb atoms, where the states $F' = 1, 2, 3$ of the hyperfine manifold $5P_{3/2}(F')$ are strongly coupled with the ground state $5S_{1/2}(F = 2)$, and the coupling is probed by a weak probing field from the other ground-state component $5S_{1/2}(F = 3)$. We present a five-level model in which the states $F = 2, 3$ and $F' = 1, 2, 3$ are taken into account, while the non-coupled state $F' = 4$ is neglected. The model is used as a starting point to reproduce spectral features observed in the absorption of probe light passing through a cold sample of ^{85}Rb atoms in a magneto-optical trap. Basing on numerical solutions of this model, we have also studied in detail the impact on the probe spectra from the presence of the state $F' = 1$ to which probing is forbidden by electric-dipole transition, but coupling is allowed [see, e.g., Proc. of SPIE **8770** (2013) 87700Q].

Keywords: electromagnetically induced transparency, Autler–Townes effect, Λ-system, cold ^{85}Rb atoms in magneto-optical trap, five-level model, master equation for the density operator

PACS: 42.50.Gy, 42.50.Hz, 31.15.xg
UDC: 535.332, 535.34

1. Introduction

If various transition paths between two states of a given system are possible, then all probability amplitudes related to these paths (or channels) should be added, instead of transition probabilities (In 1960s, Feynman has developed a so-called path integral formalism for such a case). Since the amplitudes mentioned are complex, the summations lead to a number of quantum interference effects in the system. Besides of being an interesting subject of theoretical considerations, these interference phenomena also create some possibilities for developing various systems having potential applications in nanotechnologies or quantum information technologies.

One of the most interesting aspects of the quantum interference which has been extensively studied in the last decades is electromagnetically induced transparency (EIT). In this phenomenon widely discussed in numerous studies (see, e.g., [1–6] and references cited therein), the optical properties of a medium are modified by a strong light–field coupling in such a way that the

absorption of a weak incident probe light is suppressed, or the medium becomes even completely transparent to the probe light.

The simplest system in which the EIT could be observed is a three-level system. Three levels and two light fields causing transitions among the levels can build up three basic configurations of Λ-, V-, and cascade- (or ladder-) types. However, as Abi-Salloum points out [7], the EIT-type suppression of absorption in the cascade scheme occurs only with coupling applied in the second (upper) step and, therefore, with probing in the first (lower) step (such is a scheme used e.g., in the work [5]). At the same time, the EIT does not occur at all in the V-scheme. An Autler–Townes (A-T) effect represents another phenomenon, which is different from the EIT though remains also to be related to a minimum in the profile of the probe absorption to a coupled state. The two phenomena coexist and the contribution from the EIT prevails over that originating from the A-T effect at low coupling Rabi frequencies, up to their values approximately equal to the natural linewidth. On the other hand, the A-T effect starts to dominate at the Rabi frequencies higher than these values [8–11].

In many instances, however, the approximation of a three-level atom interacting with two light fields becomes insufficient. For example, in the work [5] we have studied multiple transparency windows in view of their potential applications in slowing down light pulses at various closely lying frequencies. In order to describe the ladder scheme $5S_{1/2}(F=3) \rightarrow 5P_{3/2}(F'=3) \leftrightarrow 5P_{3/2}(F''=4,\ 3,\ 2)$, which has been applied in experiments with cold ^{85}Rb atoms in a magneto-optical trap (MOT), a model of (at least) five hyperfine-structure (hfs) levels has been necessary. The distances between the neighbouring F'' levels are comparable to the natural width of the probe absorption line in the first step, and the same is true of the Rabi frequency used for coupling in the second step. The probe beam has been scanned about the atomic resonance in the first step. With the coupling light frequency fixed inside the region of the three closely located atomic resonances of the second step, the system produces up to three EIT minima in the probe absorption profile. Following Ref. [12], a five-level model of master equation for the density operator of the considered system in a rotating wave approximation has been assumed. Although the agreement between the experimental results and the features of simulated narrow EIT effect has proved good enough, the authors have suggested its further improving by developing a model that accounts for degenerate Zeeman substates of the relevant hfs states, along with transitions among these substates.

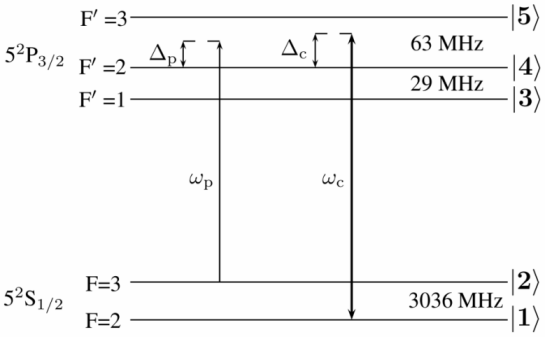

Fig. 1. A scheme of five levels of ^{85}Rb atom and transitions involved in the model adopted in the present work (not in scale). Figures from 1 to 5 correspond to hfs levels (see also ket-symbols on the r. h. s.).

In the present study we refer mainly to the results of our experiments with the cold ^{85}Rb atoms trapped in the MOT. The scheme of levels and transitions under consideration is given in

Fig. 1. Transmission spectra of a weak probe beam are detected by scanning the probe frequency (detuning Δ_p) at various fixed frequency detunings Δ_c of the coupling beam. The lower states for the coupling and probing are $5S_{1/2}(F = 2)$ and $5S_{1/2}(F = 3)$, respectively. Provided that the coupling is strong enough, all of the three hfs components of the upper state $5P_{3/2}(F' = 1, 2, 3)$ are simultaneously coupled by electric-dipole transitions. For the probing, electric-dipole transitions are allowed to the three states $5P_{3/2}(F' = 2, 3, 4)$, though we neglect the state $F' = 4$, both in the scheme of Fig. 1 and in the frame of our model (This state is not dipole-coupled and, regarding to mutual distances among the hfs states of the $5P_{3/2}$ manifold, it is the most isolated from all the other states). As a result, the number of the levels considered in this work is five, similarly to the study [5], though our scheme is different. In the title, we term this scheme of levels and transitions with multiple upper states simultaneously coupled, as a 'generalized Λ-system', to make a distinction from the actual Λ-type case related to the three-level scheme.

The article is organized as follows. In Section 2, the five-level model calculations relevant to the scheme described in the above paragraph are demonstrated. We start with the master equation for the density operator [13] for the system which consists of five atomic levels interacting with two (laser) light fields, as illustrated in Fig. 1. For simplicity, we adopt dipole and rotating wave approximations. Then a set of equations describing evolution of the density matrix elements is derived. To simulate the probe transmission spectra, the equations are solved numerically, by assuming a stationary regime. The numerical results obtained by us are compared with our earlier experimental data and discussed in Section 3. Finally, we summarize the results and make conclusions in Section 4.

2. The applied model

The scheme of the atomic states and the transitions involved in our model is given by Fig. 1.

The probe (Δ_p) and coupling (Δ_c) frequency detunings measured relative to the level |4> are defined as $\Delta_p = \omega_p - \omega_{42}$ and $\Delta_c = \omega_c - \omega_{41}$, where ω_{41} and ω_{42} denote the frequencies at the atomic resonances, and ω_p and ω_c the probe- and coupling-beam frequencies. Besides of the numbers appearing in ket-symbols on the r. h. s. of Fig. 1, there is another system of level numbering assigned to the atomic hfs levels of ^{85}Rb (see symbols on the l. h. s.):

$$|1\rangle \Rightarrow 5\,S_{1/2}(F = 2), \quad |2\rangle \Rightarrow 5S_{1/2}(F = 3), \quad |3\rangle \Rightarrow 5P_{3/2}(F' = 1),$$

$$|4\rangle \Rightarrow 5P_{3/2}(F' = 2), \quad |5\rangle \Rightarrow 5P_{3/2}(F' = 3).$$

As already mentioned in the Introduction, the transitions $|1\rangle \rightarrow |i\rangle$ ($i = 3, 4, 5$) and $|2\rangle \rightarrow |j\rangle$ ($j = 4, 5$) are dipole-allowed. The transitions among the other levels are dipole-forbidden. If the coupling laser beam is sufficiently strong, it couples state |1> with all the three states |3>, |4> and |5> at once. A weak probe-beam absorption takes place from the level |2>.

The evolution of the density operator in the dipole-interaction and rotating wave approximations is governed by the master equation for the case of a five-level atom interacting with two laser fields:

$$\frac{d\rho}{dt} = -\frac{i}{\hbar}[H, \rho] + \sum_{j=3}^{5} \Gamma_{j1} L_{j1} \rho + \sum_{j=4}^{5} \Gamma_{j2} L_{j2} \rho\,, \tag{1}$$

where the total Hamiltonian H has the form

$$H = H_0 + H_I\,. \tag{2}$$

Here H_0 is the free atomic Hamiltonian,

$$H_0 = \hbar(\Delta_p - \Delta_c)\sigma_{22} - \hbar(\Delta_c + \delta_1)\sigma_{33} - \hbar\Delta_c\sigma_{44} + \hbar(\delta_2 - \Delta_c)\sigma_{55}, \tag{3}$$

H_I the interaction Hamiltonian,

$$H_I = -\frac{\hbar}{2}\left(\sum_{j=3}^{5}\Omega_{j1}\sigma_{1j} + \sum_{j=4}^{5}\Omega_{j2}\sigma_{2j} + h.c.\right), \tag{4}$$

while $\delta_1 = \omega_{43} = 29$ MHz and $\delta_2 = \omega_{54} = 63$ MHz are the energetic distances between the states in the units of frequency (see Fig. 1). Notice that $\sigma_{ij} = |i\rangle\langle j|$ ($i, j = 1, 2, 3, 4, 5$) are the population operators for $i = j$ and the dipole operators for $i \neq j$, $\Omega_{j1} = \mu_{j1}\varepsilon_c/\hbar$ ($j = 3, 4, 5$) denotes the Rabi frequency for the coupling field and $\Omega_{j2} = \mu_{j2}\varepsilon_p/\hbar$ ($j = 4, 5$) the Rabi frequency for the probe beam, where μ_{j1} and μ_{j2} are the dipole moments for the allowed transitions. Finally, ε_c and ε_p are the electric-field amplitudes ($E_{c(p)} = \varepsilon_{c(p)}\cos\omega_{c(p)}$) for the coupling and probing fields, respectively.

The remaining terms on the r. h. s. of Eq. (1) take into account the natural decay from the state $|j\rangle$ to the states $|1\rangle$ or $|2\rangle$, with the decay rates/widths Γ_{j1} or Γ_{j2}. The operator L acts on the density matrix as follows:

$$L_{ij}\rho = \frac{1}{2}\left(2\sigma_{ji}\rho\sigma_{ij} - \sigma_{ij}\sigma_{ji}\rho - \rho\sigma_{ij}\sigma_{ji}\right). \tag{5}$$

The formulae (1)–(5) yield in the following set of equations for evolution of the density matrix elements ρ_{ij} ($i \leq j$):

$$\begin{aligned}\dot{\rho}_{11} = \frac{i}{2}\left[\Omega_{31}\left(\rho_{31} - \rho_{13}\right) + \Omega_{41}\left(\rho_{41} - \rho_{14}\right) + \Omega_{51}\left(\rho_{51} - \rho_{15}\right)\right] \\ + \Gamma_{31}\rho_{33} + \Gamma_{41}\rho_{44} + \Gamma_{51}\rho_{55},\end{aligned} \tag{6}$$

$$\begin{aligned}\dot{\rho}_{12} = \frac{i}{2}\left[-\Omega_{42}\rho_{14} - \Omega_{52}\rho_{15} + \Omega_{31}\rho_{32} + \Omega_{41}\rho_{42} + \Omega_{51}\rho_{52}\right] \\ + \left[-\gamma_{12} + i\left(\Delta_p - \Delta_c\right)\right]\rho_{12},\end{aligned} \tag{7}$$

$$\begin{aligned}\dot{\rho}_{13} = \frac{i}{2}\left[\Omega_{31}\left(\rho_{33} - \rho_{11}\right) + \Omega_{41}\rho_{43} + \Omega_{51}\rho_{53}\right] \\ - \frac{1}{2}\left[\Gamma_{31} + 2\gamma_{13} + 2i\left(\Delta_c + \delta_1\right)\right]\rho_{13},\end{aligned} \tag{8}$$

$$\begin{aligned}\dot{\rho}_{14} = \frac{i}{2}\left[-\Omega_{42}\rho_{12} + \Omega_{31}\rho_{34} + \Omega_{41}\left(\rho_{44} - \rho_{11}\right) + \Omega_{51}\rho_{54}\right] \\ - \frac{1}{2}\left[\Gamma_{41} + \Gamma_{42} + 2\gamma_{14} + 2i\Delta_c\right]\rho_{14},\end{aligned} \tag{9}$$

$$\begin{aligned}\dot{\rho}_{15} = \frac{i}{2}\left[-\Omega_{52}\rho_{12} + \Omega_{31}\rho_{35} + \Omega_{41}\rho_{45} + \Omega_{51}\left(\rho_{55} - \rho_{11}\right)\right] \\ - \frac{1}{2}\left[\Gamma_{51} + \Gamma_{52} + 2\gamma_{15} - 2i\left(\delta_2 - \Delta_c\right)\right]\rho_{15},\end{aligned} \tag{10}$$

$$\dot{\rho}_{22} = \frac{i}{2}\left[\Omega_{42}\left(\rho_{42} - \rho_{24}\right) + \Omega_{52}\left(\rho_{52} - \rho_{25}\right)\right] + \Gamma_{42}\rho_{44} + \Gamma_{52}\rho_{55}, \tag{11}$$

$$\begin{aligned}\dot{\rho}_{23} = \frac{i}{2}\left[\Omega_{42}\rho_{43} + \Omega_{52}\rho_{53} - \Omega_{31}\rho_{21}\right] \\ - \frac{1}{2}\left[\Gamma_{31} + 2\gamma_{23} + 2i\left(\delta_1 + \Delta_p\right)\right]\rho_{23},\end{aligned} \tag{12}$$

$$\dot{\rho}_{24} = \frac{i}{2}\left[\Omega_{42}\left(\rho_{44}-\rho_{22}\right)+\Omega_{52}\rho_{54}-\Omega_{41}\rho_{21}\right] - \frac{1}{2}\left[\Gamma_{41}+\Gamma_{42}+2\gamma_{24}+2i\Delta_p\right]\rho_{24}, \tag{13}$$

$$\dot{\rho}_{25} = \frac{i}{2}\left[\Omega_{42}\rho_{45}+\Omega_{52}\left(\rho_{55}-\rho_{22}\right)-\Omega_{51}\rho_{21}\right] - \frac{1}{2}\left[\Gamma_{51}+\Gamma_{52}+2\gamma_{25}+2i\left(\Delta_p-\delta_2\right)\right]\rho_{25}, \tag{14}$$

$$\dot{\rho}_{33} = \frac{i}{2}\left[\Omega_{31}\left(\rho_{13}-\rho_{31}\right)\right]-\Gamma_{31}\rho_{33}, \tag{15}$$

$$\dot{\rho}_{34} = \frac{i}{2}\left[-\Omega_{42}\rho_{32}+\Omega_{31}\rho_{14}-\Omega_{41}\rho_{31}\right]-\frac{1}{2}\left[\Gamma_{31}+\Gamma_{41}+\Gamma_{42}+2\gamma_{34}-2i\delta_1\right]\rho_{34}, \tag{16}$$

$$\dot{\rho}_{35} = \frac{i}{2}\left[-\Omega_{52}\rho_{32}+\Omega_{31}\rho_{15}-\Omega_{51}\rho_{31}\right] - \frac{1}{2}\left[\Gamma_{31}+\Gamma_{51}+\Gamma_{52}+2\gamma_{35}-2i\left(\delta_1+\delta_2\right)\right]\rho_{35}, \tag{17}$$

$$\dot{\rho}_{44} = \frac{i}{2}\left[\Omega_{42}\left(\rho_{24}-\rho_{42}\right)+\Omega_{41}\left(\rho_{14}-\rho_{41}\right)\right]-\left(\Gamma_{41}+\Gamma_{42}\right)\rho_{44}, \tag{18}$$

$$\dot{\rho}_{45} = \frac{i}{2}\left[\Omega_{42}\rho_{25}-\Omega_{52}\rho_{42}+\Omega_{41}\rho_{15}-\Omega_{51}\rho_{41}\right] - \frac{1}{2}\left[\Gamma_{41}+\Gamma_{42}+\Gamma_{51}+\Gamma_{52}+2\left(\gamma_{45}-i\delta_2\right)\right]\rho_{45}, \tag{19}$$

$$\dot{\rho}_{55} = \frac{i}{2}\left[\Omega_{52}\left(\rho_{25}-\rho_{52}\right)+\Omega_{51}\left(\rho_{15}-\rho_{51}\right)\right]-\left(\Gamma_{51}+\Gamma_{52}\right)\rho_{55}. \tag{20}$$

The forms of the other equations for $i > j$, which are dropped, come from the Hermitian property of the density operator, $\rho_{ij} = \rho_{ji}^{*}$.

The density matrix equations have been solved numerically under the steady-state condition,

$$\frac{\mathrm{d}\rho}{\mathrm{d}t} = 0, \tag{21}$$

using the relation $\mathrm{Tr}(c) = 1$ for the density operator. The absorption coefficient as a physical quantity crucial in our juxtaposition of theory and experiment, is proportional to the imaginary part of the complex electric susceptibility of the medium (Notice that the dispersion coefficient is proportional to its real part). The complex electric susceptibility is related to the relevant elements of the atomic density matrix through polarization of the medium. By following reasoning analogical to that used, e.g., in Ref. [14] for the three-level Λ-case, one can show that the probe absorption coefficient α for our case of multi-state coupling is proportional to the imaginary part of the sum in the following parenthesis,

$$\alpha \propto \mathrm{Im}\left(\mu_{24}\rho_{24}+\mu_{25}\rho_{25}\right). \tag{22}$$

The probe dispersion coefficient β is proportional to the real part of that sum,

$$\beta \propto \mathrm{Re}\left(\mu_{24}\rho_{24}+\mu_{25}\rho_{25}\right). \tag{23}$$

In this study, we are interested only in the absorption. The probe transmission T (i.e., the ratio of the intensity of the probe beam transmitted through the absorbing sample, to the intensity of the

incoming beam) is linked with the α parameter by a standard relationship $T = \exp(-\alpha l)$, with l being the path length of the probe light across the sample of absorbing cold ^{85}Rb atoms. Notice that here the absorption is meant to be the quantity $A = 1 - T$. In case of a weak absorption (i.e., small αl), the relations $T \approx 1 - \alpha l$ and $A \approx \alpha l$ hold true. With regard to Eq. (22), theoretical plots of $-\mathrm{Im}(\mu_{24}\rho_{24} + \mu_{25}\rho_{25})$ as a function of Δ_p can be compared with the corresponding experimental transmission spectra, under proper scaling. Of importance are also the points associated with the two ordinates: a theoretical point corresponding to zero absorption and an experimental one corresponding to full transmission ($T = 1$).

While solving the equations for the density matrix elements, we have adopted realistic parameters corresponding to the conditions of the experiment referred to above. Note that all the frequency values in this study are given in MHz rather than in rad/s, so that they correspond to the ordinary frequency but not the angular one.

The Rabi frequency $\Omega_{51} = 31$ MHz is evaluated from the experimental probe spectrum in the range of $\Delta_p = 63$ MHz (the probe about the atomic resonance $|2\rangle \rightarrow |5\rangle$), with Δ_c fixed at 63 MHz (the coupling at the atomic resonance $|1\rangle \rightarrow |5\rangle$). The two other coupling Rabi frequencies, $\Omega_{31} = 30.45$ MHz and $\Omega_{41} = 34.66$ MHz, are taken as being scaled from Ω_{51} according to proportions of the reduced transition-matrix elements $\langle F'||\mu||F\rangle$. It is seen that all of the three Ω values turn out to be close to each other. Much smaller values have been taken for the Rabi frequencies due to the probe field. The Γ_{ji} parameters are the rates/widths due to spontaneous fluorescence from the F' state to the F one, so that we put $\Gamma_{51} = 2.70$ MHz, $\Gamma_{52} = 3.37$ MHz, $\Gamma_{41} = 4.72$ MHz, $\Gamma_{42} = 1.35$ MHz, and $\Gamma_{31} = 6.07$ MHz. Notice that Γ_{31}, $(\Gamma_{41} + \Gamma_{42})$ and $(\Gamma_{51} + \Gamma_{52})$ are each equal to the total natural width Γ_{tot}, which is related to the natural decay of the $5P_{3/2}$ state.

In the equations of evolution for the off-diagonal elements of ρ, there are two kinds of contributions into the decoherence-related widths. Those related to Γ_{ji} (or actually to Γ_{tot}) can be expected from the form of decay terms in the Hamiltonian given by Eq. (1). On the other hand, γ_{ij} are contributions of the other kind. They are introduced directly into the equations of evolution to account for the other possible sources of decoherence. We have assumed no collisional effects in the MOT, and we consider only the influence of finite spectral widths of the probe and coupling lasers. The γ_{ij} quantities have been calculated as functions of these widths (No details of these calculations are presented here). These functions have been defined similarly as in Ref. [15]. Finally, the value of 1 MHz is taken for the spectral widths (HWHM) of the both lasers.

3. Comparison of numerical solutions with experimental spectra

As stated above, we have compared the spectra calculated in the framework of the five-level model described above, with the experimental results on the cold ^{85}Rb atoms trapped in the MOT, as described in Refs. [16, 17]. In particular, we have employed single-mode diode lasers for excitation. Some other details of the excitation/detection systems can be found in the work [18].

A selected part of transmission spectra detected in the experiment is presented in the left panels of Fig. 2a–h, while the theoretical spectra, a subject of our comparison, are given in the right panels. The horizontal axes in Fig. 2 correspond to the probe-beam detuning Δ_p defined in the Introduction. The spectra correspond to the Δ_c values −105, −60, 15, 45, 63, 70, 80, and 100 MHz. In the absence of coupling, the two atomic resonances $|2\rangle - |4\rangle$ and $|2\rangle - |5\rangle$ allowed for excitation from the ground state $|2\rangle$ would correspond to the two Lorentzian peaks in the probe absorption occurring at $\Delta_p = 0$ MHz and $\Delta_p = 63$ MHz (see dips observed in the transmission).

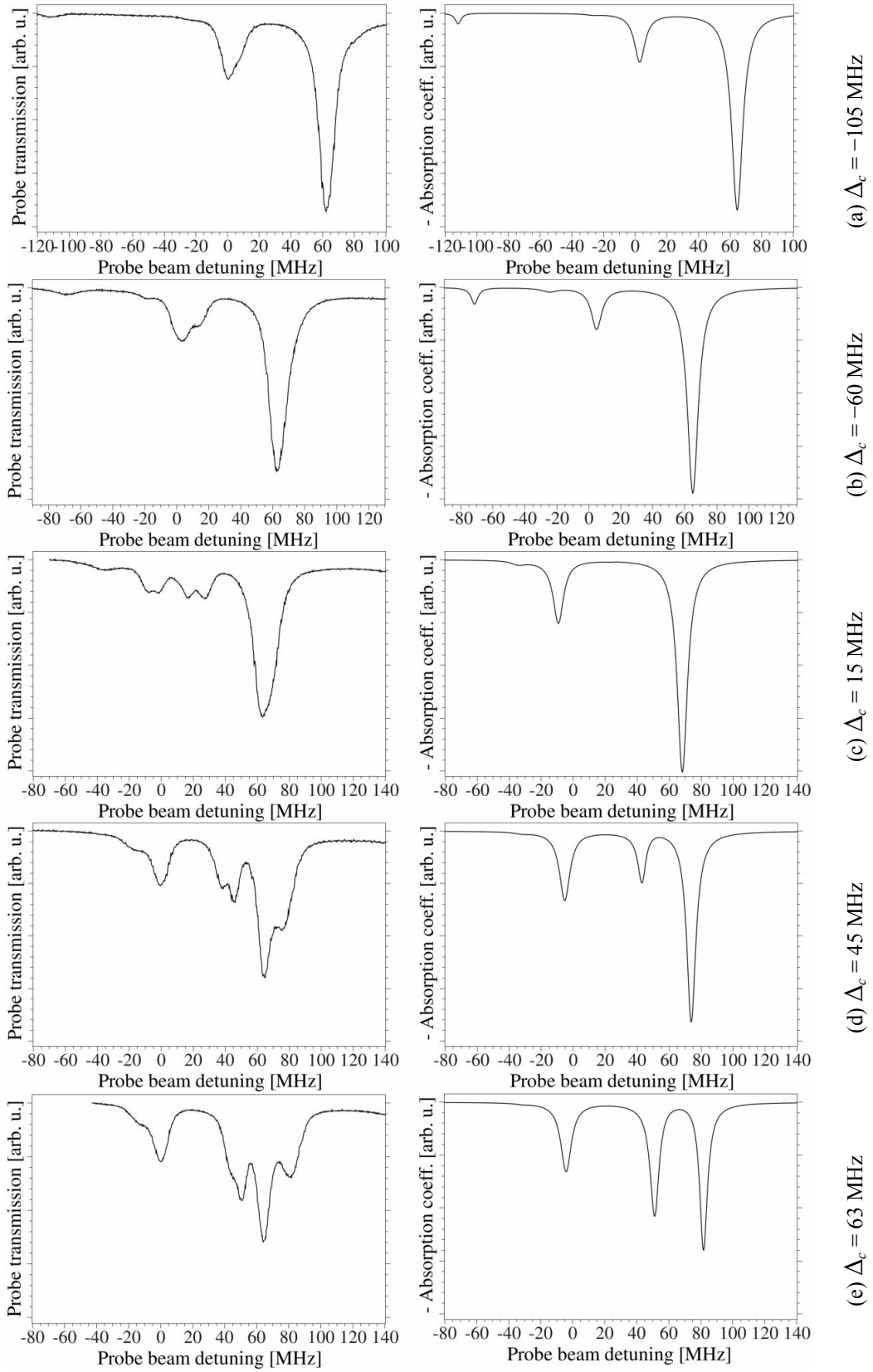
Probe transmission [arb. u.]
- Absorption coeff. [arb. u.]
Probe beam detuning [MHz]
(a) $\Delta_c = -105$ MHz
(b) $\Delta_c = -60$ MHz
(c) $\Delta_c = 15$ MHz
(d) $\Delta_c = 45$ MHz
(e) $\Delta_c = 63$ MHz

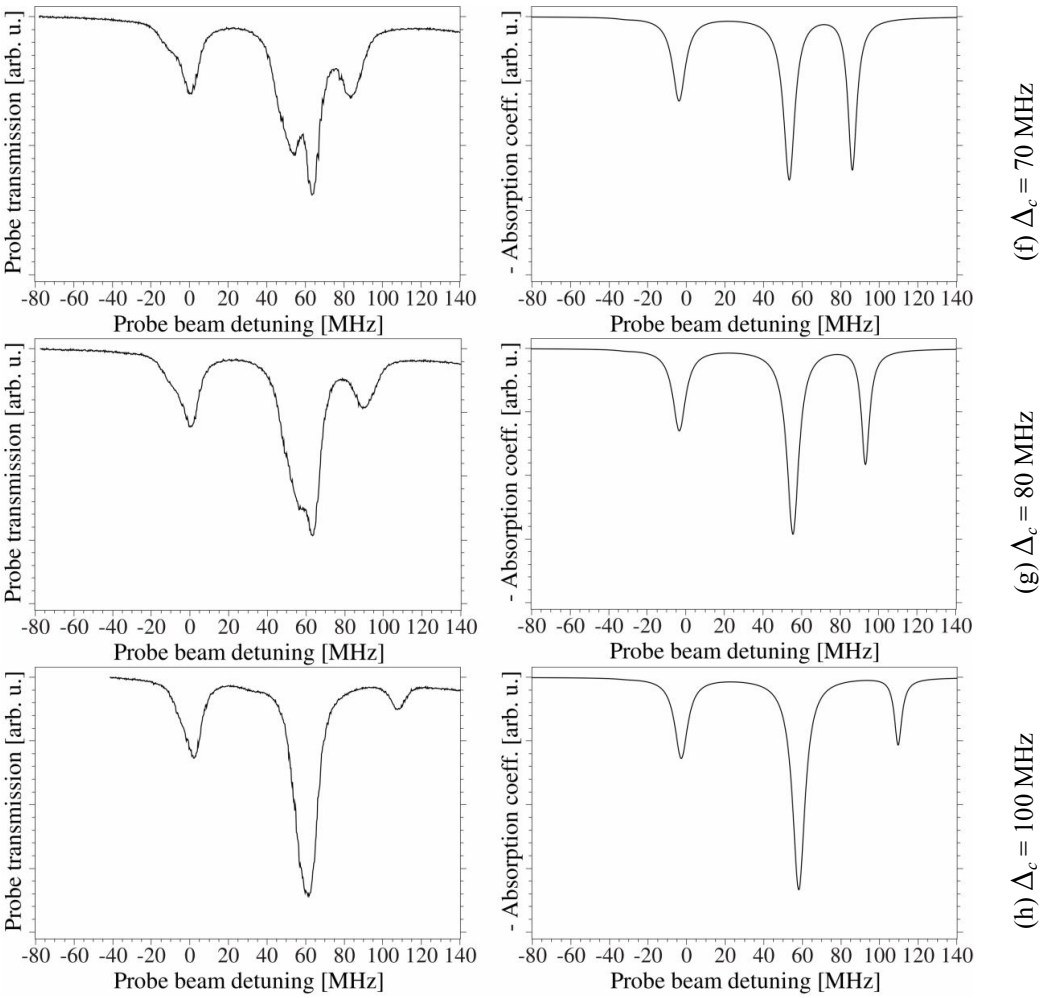

Fig. 2. Spectra calculated by assuming a five-level model described in Section 2 (r. h. s. panels) as compared with the experimental spectra (l. h. s. panels). The horizontal axes correspond to the probe beam frequency detuning Δ_p from the atomic resonance $5S_{1/2}(F = 3) \rightarrow 5P_{3/2}(F' = 2)$. The coupling beam detuning Δ_c is measured beginning from the atomic resonance $5S_{1/2}(F = 2) \leftrightarrow 5P_{3/2}(F' = 2)$. Δ_c is fixed at different values marked in the legend. Note that the total Δ_p range of 220 MHz, which is common for all panels, is shifted in panel (a).

A fairly good agreement of the theoretical and experimental spectra can be observed in Fig. 2 for the coupling frequency detuned far from the atomic resonances, i.e. in panels (a) and, perhaps, (b) (for the negative Δ_c values); the same takes place for panels (g) and, perhaps, (h) (for the positive Δ_c). However, most of the experimental spectra (even those in panels (b) and (g), and, quite obviously, the spectra displayed in all the other panels) reveal some additional absorption peaks (i.e., transmission dips), apart from the features revealed in the model spectra. This indicates that the five-level model, which refers only to the hfs transitions, is not sufficient for fully reproducing the experimental results. We attribute the 'extra' peaks to the transitions among magnetic substates, which have been neglected in the model. If we consider the transitions $(m_{F=3} - m'_{F'})$, further to the five-level configurations, some other ones can also be singled out, provided that we account for the $(m_F - m_{F'})$ selection rules with regard to the laser beam polarizations and directions (In the experiment under study, the beams have been inclined by

ca 50° and linearly polarized in the plane where the beams propagate) [19].

The influence upon formation of the spectrum from the two-level configurations is the easiest to explain. These configurations are related to absorption involving the uncoupled $m_{F'}$ states. In analogy to the cases treated in Refs. [19, 20], one can demonstrate that, among the probe absorption transitions ($m_{F=3} - m'_{F'}$) ($F' = 2$ or 3), in our five-level scheme there could exist transitions involving the $m'_{F'}$ states to which the coupling transitions are not allowed.

Such an 'uncoupled probe transition' may be considered in the framework of the two-level model, if one ignores that the other states are involved in the population distribution. Consequently, similar to a real two-level scheme, a weak absorption peak (i.e., a transmission minimum) should be centred at the corresponding atomic resonance, regardless of a fixed Δ_c value. Indeed, a peak of such an origin can be well recognized in all the experimental spectra (d)–(g) at $\Delta_p = 63$ MHz. Its presence, in the shape of an unresolved component, can also be guessed in the other panels.

As an example, let us consider the spectra in panel (e), which correspond to the coupling-beam frequency at the atomic resonance to the upper state |5> ($\Delta_c = 63$ MHz). A broad absorption minimum (a transparency window) is observed in the theoretical spectrum approximately at $\Delta_p = 63$ MHz. In connection with relatively high coupling Rabi frequency ($\Omega_{51} \approx 5\Gamma_{tot}$), one can expect that the transparency window in this work is mostly due to the A-T splitting and, to somewhat less extent, due to the EIT (see remarks in the Introduction, and references [8–11]). The very presence and the approximate position of this absorption minimum could be supposed by taking an analogy with a hypothetical three-level Λ scheme, where the state |5> plays a role of the (only) upper state. However, the exact condition $\Delta_p = \Delta_c$ in the Λ-configuration holds for Δ_p at the absorption minimum; in this case the minimum would be observed at $\Delta_p = 63$ MHz. Due to the 'concurrent' coupling of the three upper levels in our model, the minimum is shifted and some asymmetry is seen for the A-T wings. This concerns both their positions with respect to $\Delta_p = 63$ MHz and the corresponding heights. For better understanding of these points, we refer the reader to our five-level calculations with the other parameter values chosen [21, 22], the appropriate four-level calculations, our calculations with the state |3> neglected [21, 22], and those performed in Ref. [23], which have been related to D1 line of ^{133}Cs. In the experimental spectrum, the A-T wings can be recognized. Nonetheless, instead of an increased transmission at the centre, a transmission minimum is seen in between the wings at $\Delta_p = 63$ MHz, which corresponds to the absorption maximum. This has been justified above by a presence of the two-level ($m_{F=3} - m_{F'=3}$) schemes, which provide a maximum of the weak-probe absorption at the atomic resonance.

4. Summary and conclusions

In this work we present formalism and develop a model for the five hfs levels and the corresponding transitions related to a so-called D2 line of ^{85}Rb atoms. We compare the simulated spectra with the experimental ones and discuss qualitatively the origins of some of their differences. As stated above, the five-level model (plus the models strictly generated from it) serves to explain the presence and the positions of the spectral peaks observed. We realize that the calculations, which pretend to directly reproduce the exact shapes of the experimental spectra under study and to predict the spectra for any other beam directions and polarizations, should explicitly encompass all the substates m_F and $m_{F'}$ of the five hfs states under interest. A model of this kind, with greatly increased number of equations for the evolution of the density matrix elements, is just a subject of our study. In essence, the five-level model developed here has been

employed to investigate how the presence of a state, to which the coupling is allowed in the electric-dipole approximation though the probing is dipole-forbidden (such as with the $5P_{3/2}(F'=1)$ state in Fig. 1), may influence a weak probe absorption under multilevel coupling [22, 23].

The spectra have been simulated for different coupling-beam detunings Δ_c, as well as for the Rabi frequencies Ω_c varying in a considerably wide region. Even in cases of comparatively low Rabi frequencies close to the natural width and, in particular, of increased Ω_c, the main features of the probe spectra depend substantially upon a presence of the state, which is dipole-coupled but not dipole-probed. This result importantly indicates that the omission of such a state in modelling may have led to wrong predictions. We also notice that the results of Ref. [22] assuming negligible decoherence widths γ_{ij} may be of interest in developing quantum memory protocols [23], e.g., at the level of decisions about atomic schemes to be considered.

References

1. Imamoglu A and Harris S E, 1989. Lasers without inversion: interference of dressed lifetime-broadened states. Opt. Lett. **14**: 1344−1346.
2. Fleischhauer M, Imamoglu A and Marangos J P, 2005. Electromagnetically induced transparency: optics in coherent media. Rev. Mod. Phys. **77**: 633−673.
3. Harris S E, 1997. Electromagnetically induced transparency. Phys. Today. **50**: 36−42.
4. Harris S E and Hau L V, 1999. Nonlinear optics at low light levels. Phys. Rev. Lett. **82**: 4611−4614.
5. Kowalski K, Cao Long V, Nguyen Viet H, Gateva S, Głódź M and Szonert J, 2009. Simultaneous coupling of three hfs components in cascade scheme of EIT in cold ^{85}Rb atoms. J. Non-Cryst. Solids. **355**: 1295−1301.
6. Kowalski K, Cao Long V, Dinh Xuan K, Głódź M, Nguyen Huy B and Szonert J, 2010. Electromagnetically induced transparency. Comput. Meth. Sci. Technol. Special issue: 131−145.
7. Abi-Salloum T Y, 2010. Electromagnetically induced transparency and Autler-Townes splitting: Two similar but distinct phenomena in two categories of three-level atomic systems. Phys. Rev. A. **81**: 053836.
8. Li Y Q and Xiao M, 1995. Electromagnetically induced transparency in a three-level Λ−type system in rubidium atoms. Phys. Rev. A. **51**: R2703−R2706.
9. Li Y Q and Xiao M, 1995. Observation of quantum interference between dressed states in an electromagnetically induced transparency. Phys. Rev. A. **51**: 4959−4962.
10. Anisimov P M, Dowling J P and Sanders B C, 2011. Objectively discerning Autler-Townes splitting from electromagnetically induced transparency. Phys. Rev. Lett. **107**: 163604.
11. Giner L, Veissier L, Sparkes B, Sheremet A S, Nicolas A, Mishina O S, Scherman M, Burks S, Shomroni I, Kupriyanov D V, Lam P K, Giacobino E and Laurat J, 2013. Experimental investigation of the transition between Autler-Townes splitting and electromagnetically-induced-transparency models. Phys. Rev. A. **87**: 013823.
12. Wang J, Kong L B, Tu X H, Jiang K J, Li K, Xiong H W, Zhu Y and Zhan M S, 2004. Electromagnetically induced transparency in multi-level cascade scheme of cold rubidium atoms. Phys. Lett. A. **328**: 437−443.
13. Scully M O and Zubairy M S, Quantum optics. Cambridge: Cambridge University Press (1997).

14. Gea-Banacloche J, Li Y Q, Jin S Z and Xiao M, 1995. Electromagnetically induced transparency in ladder-type inhomogeneously broadened media: Theory and experiment. Phys. Rev. A. **51**: 576−584.
15. Petch J C, Keitel C H, Knight P L and Marangos J P, 1996. Role of electromagnetically induced transparency in resonant four-wave-mixing schemes. Phys. Rev. A. **53**: 543−561.
16. Kowalski K, Dimova-Arnaudova E, Fronc K, Gateva S, Głódź M, Lis L, Petrov L and Szonert J, 2006. A system for magnetooptical cooling and trapping of Rb atoms. Opt. Appl. **36**: 559−567.
17. Kowalski K, Cao Long V, Dinh Xuan K, Głódź M, Nguyen Huy B and Szonert J, 2010. Magneto-optical trap: fundamentals and realization. Comput. Meth. Sci. Technol. Special issue: 115−129.
18. Kowalski K, Vaseva K, Gateva S, Głódź M, Petrov L and Szonert J, 2007. System for EIT spectroscopy of cold Rb atoms. Proc. SPIE. **6604**: 6604K.
19. Chen Y-Ch, Lin Chi-W and Yu I A, 2000. Role of degenerate Zeeman levels in electromagnetically induced transparency. Phys. Rev. A. **61**: 053805.
20. Park S J, Kwon T Y and Lee H S, 2004. Effects of coherent uncoupled excited states on electromagnetically induced transparency. Japan. J. Appl. Phys. **43**: 7273−7276.
21. Żaba A, Paul-Kwiek E, Kowalski K, Szonert J, Woźniak D, Gateva S, Cao Long V and Głódź M, 2013. The role of a dipole-coupled but not dipole-probed state in probe absorption with multilevel coupling (accepted for publication in Eur. Phys. J., Special Topic).
22. Żaba A, Paul-Kwiek E, Kowalski K, Szonert J, Woźniak D, Gateva S, Cao Long V and Głódź M, 2013. Pump-probe spectra modeled with inclusion of a dipole-coupled but not dipole-probed F' state, for the case of ^{85}Rb $5S_{1/2}(F)\leftrightarrow 5P_{3/2}(F')$ transitions. Proc. SPIE. **8770**: 87700Q.
23. Sheremet A S, Gerasimov L V, Sokolov I M, Kupriyanov D V, Mishina O S, Giacobino E and Laurat J, 2010. Quantum memory for light via a stimulated off-resonant Raman process: beyond the three-level Λ-scheme approximation. Phys. Rev. A. **82**: 033838.

Żaba A., Cao Long V., Głódź M., Paul-Kwiek E., Kowalski K., Szonert J., Woźniak D. and Gateva S. 2013. Electromagnetically induced transparency and Autler–Townes effect in a generalized Λ-system: A five-level model. Ukr.J.Phys.Opt. **14**: 135 – 145.

Анотація. *У цій роботі розраховано діелектричну сприйнятність лазерно сформованого атомарного середовища. Застосована модель відповідає експериментові з холодними атомами ^{85}Rb, де стани $F' = 1, 2, 3$ надтонкої множини $5P_{3/2}(F')$ сильно зв'язані з основним станом $5S_{1/2}$ $(F = 2)$, а зв'язок тестується компонентою слабкого зондувального поля іншого основного стану $5S_{1/2}$ $(F = 3)$. Нами представлено п'ятирівневу модель, яка враховує стани $F = 2, 3$ і $F' = 1, 2, 3$ і нехтує незв'язаним станом $F' = 4$. Цю модель використано як базову для відтворення спектральних характеристик, що виявляються в поглинанні зондувального світлового випромінювання, яке поширюється крізь холодні атоми ^{85}Rb у магнітооптичній пастці. На основі чисельного розв'язку в рамках цієї моделі ми також докладно вивчили вплив на спектр зондування присутності стану $F' = 1$, для якого допускається зв'язок, однак електродипольні переходи заборонено [див., наприклад, Proc. SPIE **8770** (2013) 87700Q].*